



Published in final edited form as:

Cancer Res. 2019 December 01; 79(23): 5920–5929. doi:10.1158/0008-5472.CAN-19-1405.

BRCA1 Deficiency Upregulates NNMT Which Reprograms Metabolism and Sensitizes Ovarian Cancer Cells to Mitochondrial Metabolic Targeting Agents

Arun Kanakkanthara^{1,2}, Kiran Kurmi², Thomas L. Ekstrom¹, Xiaonan Hou¹, Emma R. Purfeerst¹, Ethan P. Heinzen³, Cristina Correia¹, Catherine J. Huntoon¹, Daniel O'Brien³, Andrea E. Wahner Hendrickson¹, Sean C. Dowdy⁴, Hu Li², Ann L. Oberg³, Taro Hitosugi^{1,2}, Scott H. Kaufmann^{1,2}, S. John Weroha¹, Larry M. Karnitz^{1,2}

¹Department of Oncology, Mayo Clinic, Rochester, Minnesota

²Department of Molecular Pharmacology and Experimental Therapeutics, Mayo Clinic, Rochester, Minnesota

³Division of Biomedical Statistics and Informatics, Mayo Clinic, Rochester, Minnesota

⁴Division of Gynecologic Surgery, Mayo Clinic, Rochester, Minnesota

Abstract

BRCA1 plays a key role in homologous recombination (HR) DNA repair. Accordingly, changes that downregulate BRCA1, including BRCA1 mutations and reduced BRCA1 transcription, due to promoter hypermethylation or loss of the BRCA1 transcriptional regulator CDK12, disrupt HR in multiple cancers. In addition, BRCA1 has also been implicated in the regulation of metabolism. Here, we showed that reducing BRCA1 expression, either by CDK12 or BRCA1 depletion, led to metabolic reprogramming of ovarian cancer cells, causing decreased mitochondrial respiration and reduced ATP levels. BRCA1 depletion drove this reprogramming by upregulating NNMT (nicotinamide N-methyltransferase). Notably, the metabolic alterations caused by BRCA1 depletion and NNMT upregulation sensitized ovarian cancer cells to agents that inhibit mitochondrial metabolism (VLX600 and tigecycline) and to agents that inhibit glucose import (WZB117). These observations suggest that inhibition of energy metabolism may be a potential strategy to selectively target BRCA1-deficient high-grade serous ovarian cancer (HGSOC), which is characterized by frequent BRCA1 loss and NNMT overexpression.

Keywords

High-grade serous ovarian cancer; BRCA1; NNMT; mitochondrial metabolism; VLX600; tigecycline

To whom correspondence should be addressed: Larry M. Karnitz, Division of Oncology Research, Gonda 19-300, Mayo Clinic, 200 First Street SW, Rochester, MN 55905. Telephone: 507-284-3124; karnitz.larry@mayo.edu.

Present Address: Kiran Kurmi, Harvard Medical School, Boston MA 02115, USA.

Conflict of interest statement: A. Kanakkanthara and L. M. Karnitz are co-inventors on a provisional patent application related to the findings in this manuscript. The other authors declare no potential conflicts of interest.

INTRODUCTION

Ovarian cancer is the leading cause of death from gynecological malignancies. Patients with high-grade serous ovarian cancer (HGSOC), the most common and aggressive histotype, have a 5-year survival of only 20–30% (1). HGSOC is characterized by defects in homologous recombination (HR) repair that primarily arise from mutations in genes that encode *BRCA1*, *BRCA2* and at least 11 other HR proteins. In a smaller subset of HGSOCs, HR defects reflect transcriptional repression of *BRCA1* resulting from hypermethylation of the *BRCA1* promoter or mutational inactivation of cyclin dependent kinase 12 (CDK12), which regulates transcription of *BRCA1* and other genes involved in DNA repair (2,3). Notably, deleterious *BRCA1* and *BRCA2* mutations are associated with better outcomes in patients treated with platinum-based therapies and poly(ADP-ribose) polymerase (PARP) inhibitors due to the defects in HR repair (4).

Despite recent therapeutic advances seen with PARP inhibitors in HGSOC (5), new treatment options are still needed for this disease. One potential alternative target is reprogrammed tumor metabolism, which is emerging as a metabolic liability in many cancers (6,7). Intriguingly, *BRCA1* has recently been shown to regulate metabolism, and *BRCA1* deficiency was shown to reduce mitochondrial oxygen consumption in breast cancer cells and skeletal muscle (8–10). These observations suggest that, in addition to its role in HR, *BRCA1* also plays a key role in the regulation of mitochondrial metabolism. However, the mechanism by which *BRCA1* loss reprograms tumor metabolism is unknown. Moreover, it is unclear whether *BRCA1* deficiency also affects mitochondrial metabolism in HGSOC.

Nicotinamide N-methyltransferase (NNMT) has also emerged as a regulator of metabolism. NNMT catalyzes the transfer of methyl groups from S-adenosyl methionine (SAM) to nicotinamide, effectively increasing N1-methylnicotinamide levels and reducing SAM levels. Although it is not fully understood how NNMT expression affects cell metabolism, several studies have demonstrated that NNMT alters energy homeostasis in mice and that NNMT overexpression decreases oxygen consumption in adipocytes and hepatoma cells (11). Interestingly, NNMT is overexpressed in many tumors (12), including HGSOC (13,14). In addition, depletion of NNMT blocks the proliferation of ovarian cancer cell lines selected to proliferate during metabolic stress induced by low glucose (13). Although these observations suggest that NNMT plays a role in ovarian cancer energy metabolism, it is not known whether NNMT affects sensitivity to metabolic inhibitors.

Here, we report that loss of *BRCA1*, induced by downregulation of either *BRCA1* or CDK12, impairs mitochondrial respiration and reduces ATP levels. Notably, these metabolic changes are dependent on and phenocopied by NNMT overexpression, indicating that NNMT drives the metabolic remodeling. Consistent with the emerging idea that targeting mitochondrial dysfunction and/or tumor metabolism is a promising therapeutic approach to selectively kill metabolically defective tumor cells (6,7), we find that *BRCA1* depletion or NNMT overexpression confers sensitivity to agents that inhibit glucose transport and mitochondrial oxidative phosphorylation (OXPHOS), including agents that are in clinical trials as well as FDA-approved drugs that might be repurposed. Collectively, our data

suggest that metabolic changes induced by *BRCA1* dysfunction and NNMT overexpression might be therapeutically exploited in BRCA1-deficient or NNMT-overexpressing HGSOC.

MATERIALS AND METHODS

Cell lines, cell culture, and metabolism-targeting agents

OVCAR-8 and OVCAR-5 cells were kind gifts from D. Scudiero (NCI, National Institutes of Health). The PEA1 cell line was from Sigma-Aldrich. The *BRCA1*-mutant COV362 cell line was a gift from Robert van Waardenburg, University of Alabama Birmingham. The cells were cultured in RPMI-1640 medium (Corning) supplemented with 8% fetal bovine serum (Millipore), and maintained in a humidified 37°C, 5% CO₂ incubator. All cells were authenticated by autosomal STR profiling (University of Arizona Genetics Core). All cell lines were free of *Mycoplasma* contamination as determined testing with a MycoAlert Mycoplasma Detection Kit (Lonza). VLX600 was obtained from Cayman Chemical. Tigecycline and WZB117 were obtained from Selleck Chemicals.

siRNAs and siRNA transfection

All siRNAs were purchased from Dharmacon. The siRNA sequences are listed in Supplementary Materials and Methods. siRNA (20 µL of 20 µM siRNA/transfection) was mixed with $5-8 \times 10^6$ cells in 180 µL media in 4-mm cuvette and electoporated with a BTX ECM 830 electroporator with two, 280-volt, 10-msec pulses).

Plasmids, plasmid transfection, and stable cell line generation

A mammalian expression plasmid that encoded human NNMT fused to Myc and DDK tags at its C terminus was obtained from Origene (Cat# RC200641). For the generation of stable NNMT overexpressing OVCAR-8 cell lines, the NNMT-Myc-DDK plasmid or empty vector control was transfected (5 µg/transfection) into OVCAR-8 cells (8×10^6 cells/transfection) using a BTX ECM 830 electroporator (using a 4-mm cuvette with two, 280-volt, 10-msec pulses). Cells were plated in 10-cm dishes containing RPMI supplemented with 8% fetal bovine serum and incubated for 48 h. After G418 (2 mg/mL) was added, the cells were cultured for an additional 12 days, replenishing the selection medium every 3 days. G418-resistant clones were trypsinized using 0.25% Trypsin-EDTA (Life Technologies) and reseeded at 50 cells per dish into 15-cm dishes containing 2 mg/mL G418. After 10 days of culture, single colony clones were picked, expanded in 24-well plates containing complete medium plus G418. Seven to 10 days later, 10 empty vector or NNMT cell clones were isolated and assayed for NNMT by immunoblotting for each stably transfected cell line. To generate the SFB-BRCA1 mammalian expression plasmid, human full-length *BRCA1* cDNA (15) was subcloned into the pSFB vector that contains in-frame N-terminal S-peptide, FLAG, and streptavidin-binding peptide tags (16). For the generation of stable BRCA1 overexpressing COV362 cells, the SFB-BRCA1 plasmid or empty vector control plasmid was transfected (40 µg/transfection) into COV362 cells (10×10^6 cells/transfection), and after 48 h, the cells were cultured for an additional 21 days with G418 (1 mg/mL), replenishing the selection medium every 3 days. The G418-resistant cells were used for subsequent experiments.

Immunoblotting

Forty-eight hours after siRNA transfection, cells were harvested and lysed in 50 mM HEPES, pH 7.6, 150 mM NaCl, 1 mM EDTA, 1% Triton X-100, 10 mM NaF, 30 mM sodium pyrophosphate, 1 mM Na₃VO₄, 10 mM 2-glycerophosphate, 10 µg/mL leupeptin, 5 µg/mL aprotinin, 5 µg/mL pepstatin, and 20 mM microcystin-LR. Immunoblotting was done using the following primary antibodies: mouse monoclonal CDK12, which was generated in our laboratory (Clone 1.11.1 B9, 1:100); mouse monoclonal BRCA1 (1:2000, sc-6954, Santa Cruz Biotechnology); rabbit polyclonal BRCA2 (1:5000, A303–434A, Bethyl Laboratories Inc.); mouse monoclonal NNMT (1:5000, ab119758, Abcam); rabbit polyclonal RAD51 (1:2000, PC-130, Calbiochem); rabbit polyclonal tubulin (1:1000, 2144S, Cell Signaling Technology); rabbit monoclonal DYKDDDK (recognizes same sequence as FLAG®, 1:1000, 14793, Cell Signaling Technology); mouse monoclonal FLAG (F1804, Sigma); and mouse monoclonal HSP90 (1:1000; D. Toft, Mayo Clinic, H9010). Secondary antibodies used were: horseradish peroxidase-conjugated anti-mouse immunoglobulin G (1:10,000 for CDK12, 1:2000 for BRCA1, and 1:20,000 for NNMT and HSP90, #7076S, Cell Signaling Technology) and anti-rabbit immunoglobulin G (1:5,000 for BRCA2 and DYKDDDK and 1:10,000 for RAD51 and tubulin, #7074S, Cell Signaling Technology).

Quantitative real-time PCR (qPCR)

Total RNA isolation from cells was performed using a miRNeasy mini kit (Qiagen) following the supplier's instructions. cDNA was synthesized from 1 µg of total RNA using oligo(dT) primers and SuperScript™ III reverse transcriptase (ThermoFisher Scientific). qPCR was performed in triplicate for each sample (25 ng cDNA template in a final volume of 20 µL) on a CFX96 real-time PCR system (Bio-Rad) using iTaq Universal SYBR Green Supermix (Bio-Rad). mRNA expression was normalized to GAPDH. The qPCR primers used are listed in Supplementary Materials and Methods.

Clonogenic assays

Two days after siRNA transfection, cells were seeded in 6-well plates at 300 cells/well for OVCAR-8 and 600 cells/well for PEA1 in triplicate and allowed to adhere overnight. The stable OVCAR-8-EV or OVCAR-8-Myc-DDK-NNMT cells were seeded at 300 cells/well. One day after plating, VLX600, tigecycline, or WZB117 was added at the indicated concentrations, the cells were culture for 8–10 days in the continued presence of the agents. Colonies were stained with Coomassie Blue, and colonies of >50 cells were counted manually. Inhibition of colony formation was presented as percentage of colonies formed in corresponding untreated control.

Cell Proliferation Assay

Cell proliferation was assessed with the CyQUANT® Cell Proliferation Assay kit (ThermoFisher Scientific). siRNA-transfected OVCAR-8 cells or stable OVCAR-8-EV or OVCAR-8-Myc-DDK-NNMT cells were plated at 4000 cells/well in flat-bottom 96-well plates, and analyzed 24, 48, and 72 h after plating following the supplier's instructions.

Chromatin immunoprecipitation (ChIP) Assays

Cells (1×10^7) in 15-cm dishes were cross-linked with 1% formaldehyde in media for 10 min at room temperature, and the unreacted formaldehyde was quenched by adding 1/10 volume 1.25 M glycine (pH 7.0). The cells were harvested by trypsinization, washed with PBS, and re-suspended in cell lysis buffer (10 mM Tris, HCl, pH 7.5, 10 mM NaCl, 0.5% NP-40). After incubation on ice for 15 min, the chromatin fraction (pellet) was collected by centrifugation at $800 \times g$ for 5 min at 4°C, digested with micrococcal nuclease (2.5 units/ml; New England Biolabs) for 20 min at 37°C, and sonicated for 15 min. Aliquots of sheared chromatin were immunoprecipitated using protein G Dynabeads™ and 2 µg of mouse monoclonal BRCA1 (sc-6954, Santa Cruz Biotechnology) or mouse monoclonal FLAG (F1804, Sigma) antibodies. Normal mouse IgG (2 µg/ChIP, 0107-01, SouthernBiotech) was used as negative control. After immunoprecipitation, crosslinks were reversed by heating to 60°C, and immunoprecipitated DNA was purified using spin columns (Cat. No. 11732676001, Roche). qPCR analysis of the immunoprecipitated and genomic input DNAs was performed using iQ™ SYBR® Green Supermix (Bio-Rad). The following primers that amplify the *NMT* promoter region were used: forward, 5'-CACTGCCTGTCTCTGACCAA-3' and reverse, 5'-CAGGAGAACAGGGCTGAAAG-3'.

Mitochondrial DNA copy number analysis

OVCAR-8 cells (8×10^6) were transfected with non-targeting control, BRCA1, or CDK12 siRNAs. Two days after transfection, genomic DNA was extracted using the Wizard® SV Genomic DNA Purification System (Promega). The relative number of copies of mitochondrial DNA were measured using the human mitochondrial DNA monitoring primer set (Cat. No. 7246; Takara) and normalized using nuclear DNA content following the supplier's protocol.

ATP and ADP assays

Forty-eight hour after siRNA transfection, total ATP and ADP levels in the cells were measured using colorimetric ATP assay (Cat. No. ab83355, Abcam) and ADP Assay (Cat. No. ab83359, Abcam) kits.

HGSOC tumor tissues

All HGSOC tumor tissues that were used in the *ex vivo* culture studies, mRNA expression studies, and protein expression studies were obtained in accord with the U.S. Common Rule after written informed consent was obtained under an active Mayo Clinic Institutional Review Board-approved banking protocol.

Ex vivo culture of HGSOC tumor tissues from PDX mouse models

All HGSOC tumor tissues were collected under an active protocol approved by the Mayo Clinic Institutional Review Board as described above. In compliance with the Health Insurance Portability and Accountability Act, all samples were first coded with a unique participant ID number with restricted access to the master key limited to authorized personnel of Mayo Clinic Ovarian Tumor Repository. To further protect patient confidentiality, PDX tumors were coded with a patient heterotransplant (PH) number for

end-users of PDX models while the Repository maintains a secure link back to participant ID numbers.

For short-term *ex vivo* monolayer cultures of tumor cells, HGSOC tissues from PDX mouse models were harvested, minced into 2–4-mm pieces, and dissociated using a Tumor Dissociation Kit (Cat. #130–096-730, Miltenyi Biotec) following the supplier's protocol. The dissociated cells were washed 5 times with RPMI-1640 medium (Invitrogen) supplemented with 10% fetal bovine serum (Invitrogen), 100 units/mL penicillin, and 100 units/mL streptomycin (Invitrogen). After resuspending in RPMI-1640 medium with 10% fetal bovine serum without antibiotics, the cells were electroporated with control luciferase (Luc), non-targeting siRNA #3, BRCA1, or CDK12 siRNAs as described above. The cells were then plated in 24-well plates in RPMI-1640 supplemented with 10% fetal bovine serum with antibiotics, cultured for 48 h, and analyzed for ATP content using a colorimetric ATP assay (Cat. No. ab83355, Abcam) and BRCA1 and CDK12 mRNA levels by qRT-PCR.

Correlation analyses of BRCA1 and CDK12 versus NNMT in patient and PDX tumors

All HGSOC tumor tissues were collected under an active protocol approved by the Mayo Clinic Institutional Review Board as described above. *CDK12*, *BRCA1*, and *NNMT* mRNA levels were obtained from an expression analysis in 98 HGSOC patient tumors and 127 non-overlapping HGSOC PDX models grown in mice. All animal studies and procedures were reviewed and approved by the Mayo Clinic Institutional Animal Care and Use Committee (IACUC). To assess the correlation between *NNMT* mRNA levels with *CDK12* and *BRCA1*, Spearman correlation analysis was performed.

Seahorse assay

Twenty-four hour after siRNA transfection, OVCAR-8 or PEA1 cells were plated at 8,000 or 7,000 cells/well, respectively, onto Seahorse 8-well XFp cell culture miniplates and allowed to grow for another 24 h before being assayed for oxygen consumption rate (OCR) and extracellular acidification rate (ECAR) on a Seahorse XFp extracellular flux analyzer (Seahorse Bioscience, Agilent Technologies). One hour prior to the start of the assay, cells were washed and changed to Seahorse XF base assay medium supplemented with 2 mM L-glutamine and 10 mM glucose, adjusted to pH 7.4, and incubated in a 37°C non-CO₂ incubator. OCR was measured using the Seahorse XFp Cell Mito Stress Test Kit (Agilent Technologies) under basal conditions and after the sequential addition of 1 μM oligomycin, 0.5 μM carbonyl cyanide p-trifluoromethoxyphenylhydrazone (FCCP), and 0.5 μM rotenone and antimycin A. ECAR was measured under basal conditions and after sequential injections of 10 mM glucose, 2.5 μM oligomycin and 50 mM 2-deoxy-glucose. OCR and ECAR measurements were taken at three time points before and after the addition of each inhibitor. Experiments were repeated three times, with 2 or more samples per experimental point.

Accession number

The RNA-seq count data have been deposited in the Gene Expression Omnibus database under accession number GSE138288.

RESULTS AND DISCUSSION

CDK12 depletion disrupts mitochondrial metabolism, reducing respiration but not glycolysis

While assessing how loss of CDK12 affects ovarian cancer cells, we observed that CDK12 depletion reduced ATP levels in OVCAR-8 and PEA1 cells (Fig. 1A, Supplementary Fig. S1A), with corresponding increases in ADP levels (Supplementary Fig. S1B). Because ATP is produced primarily by OXPHOS or glycolysis (17), we profiled the metabolic activity of these cells using extracellular flux analyses to determine whether CDK12 depletion affected either process. These studies showed that the extracellular acidification rate (ECAR), an indicator of glycolysis, was not reduced by CDK12 depletion (Supplementary Fig. S1C). In contrast, the oxygen consumption rate (OCR), an indicator of OXPHOS, was reduced under basal conditions (Fig. 1B) as well as after treatment with oligomycin, an inhibitor of ATP synthase; carbonyl cyanide p-trifluoromethoxyphenylhydrazone (FCCP), an uncoupler of mitochondrial oxidative phosphorylation; and rotenone and antimycin A, two inhibitors of mitochondrial electron transport complexes I and II, respectively (18). These findings demonstrate that CDK12 depletion reprograms mitochondrial metabolism, leading to reduced OCR and ATP production.

Metabolic reprogramming induced by CDK12 depletion is phenocopied by BRCA1 depletion

Studies from our lab and others have shown that CDK12 depletion reduces BRCA1 expression (2,3). Because BRCA1 defects have previously been shown to reduce mitochondrial oxygen consumption in breast cancer cells (9), we asked whether the mitochondrial respiration defects induced by CDK12 loss may actually be caused by loss of BRCA1. Consistent with this possibility, BRCA1 depletion also reduced OCR (Fig. 1C) and ATP production (Supplementary Fig. S1A) without disrupting glycolysis (Supplementary Fig. S2A and B). Similarly, depletion of CDK12 and BRCA1 reduced ATP levels in *ex vivo*-cultured HGSOC patient-derived xenografts (Supplementary Fig. S2C and D), indicating that this effect was not unique to cell lines. In agreement with these findings, BRCA1 re-expression in BRCA1-deficient COV362 ovarian cancer cells increased OCR (Supplementary Fig. S2E). The reduced OCR and ATP levels caused by CDK12 or BRCA1 depletion were not the result of reduced mitochondrial number, as determined by mitochondrial DNA copy number (Supplementary Fig. S2F), suggesting that they stem from decreased flux through electron transport complexes rather than a decrease in mitochondria. Taken together, these results demonstrate that BRCA1 regulates OCR and ATP levels in ovarian cancer cells.

Finally, we addressed whether the OCR reduction caused by CDK12 depletion was driven by the corresponding loss of BRCA1. This analysis showed that re-expression of exogenous BRCA1 in CDK12-depleted cells restored OCR in CDK12-depleted cells (Fig. 1D; Supplementary Fig. S2G and H), thus demonstrating that the BRCA1 loss caused by CDK12 depletion drives metabolic reprogramming.

Disabling HR does not cause the mitochondrial dysfunction induced by BRCA1 depletion

Because BRCA1 plays a central role in HR DNA repair (19), we next asked whether an HR defect induced by loss of other HR proteins would similarly cause the mitochondrial defect induced by BRCA1 depletion. In contrast to what was observed with BRCA1 depletion, depletion of BRCA2, a key participant in HR, did not cause defects in OCR (Supplementary Fig. S3A) but did disrupt HR, as shown by increased sensitivity to the PARPi olaparib (Supplementary Fig. S3B). Similar results were seen with RAD51 depletion, which did not affect OCR but did sensitize to olaparib (Supplementary Fig. S3C and D). Taken together, these results suggest that the role of BRCA1 in metabolism is independent of its role in HR and support a model in which BRCA1 deficiency reprograms mitochondrial metabolism in ovarian cancer.

Upregulation of NNMT drives the metabolic alteration caused by BRCA1 depletion

To gain insight into how CDK12 and BRCA1 depletion affected mitochondrial respiration, we analyzed an RNA-seq dataset from control and CDK12-depleted OVCAR-8 cells (Supplementary Table 1). Consistent with previously published RNA-seq analyses (3,20), CDK12 depletion altered the expression of genes involved in DNA replication, DNA repair, RNA processing, and RNA splicing (Supplementary Table 1). However, we also noticed that NNMT mRNA levels were increased ~4 fold in the CDK12-depleted cells (Supplementary Table 1). Because NNMT has been implicated in mitochondrial energy metabolism (11,13,21), and it is frequently overexpressed in multiple cancers (12), including HGSOc (13,14), we asked 1) whether BRCA1 levels affected NNMT levels in cell lines and human tumors, and 2) whether NNMT overexpression could drive the decrease in OCR.

To explore these questions, we first demonstrated that two independent BRCA1 siRNAs which target two different exons and suppress expression of multiple forms of BRCA1 mRNAs (Supplementary Fig. S4A and B), increased NNMT mRNA and protein levels in multiple ovarian cancer cell lines (Fig. 2A; Supplementary Fig. S4C). Consistent with the cell line studies, NNMT mRNA and BRCA1 mRNA levels were inversely correlated in HGSOc patient tumors and in tumors grown in patient-derived xenograft models (Fig. 2B, left two panels). Similarly, NNMT protein levels were also inversely correlated with BRCA1 mRNA and CDK12 protein levels in HGSOc tumors (Fig. 2B, right two panels; Supplementary Table 2). Second, to determine if BRCA1 loss drives these metabolic effects by upregulating NNMT, we co-depleted NNMT and BRCA1 and found that NNMT depletion reversed the OCR defect caused by BRCA1 depletion (Fig. 2C). Moreover, we also found that BRCA1, which is known to regulate gene transcription, occupies the *NNMT* promoter (Supplementary Fig. S4D and E). Finally, we observed that transient overexpression of NNMT reduced OCR (Fig. 2D). Taken together, these results demonstrate that BRCA1 occupies the *NNMT* promoter and regulates NNMT expression. Additionally, these results show that NNMT is both necessary and sufficient to reprogram mitochondrial metabolism in ovarian cancer cells.

BRCA1 depletion sensitizes ovarian cancer cells to mitochondrial metabolic targeting agents

Because BRCA1 depletion disrupted mitochondrial respiration and reduced ATP levels (Fig. 1C; Supplementary Fig. S1A and S2C), we reasoned that BRCA1-deficient cells would be more sensitive to agents that cause additional metabolic stress. To test this possibility, we assessed the effect of several small molecules that inhibit energy metabolism. These include: 1) VLX600, an iron chelator that targets metabolically compromised tumors by causing mitochondrial dysfunction and inhibiting mitochondrial respiration (7); 2) tigecycline, an FDA-approved antibiotic that inhibits mitochondrial protein translation (22); and 3) WZB117, which inhibits the glucose transporter GLUT1 and reduces intracellular ATP levels (23). As shown in Fig. 3, BRCA1 depletion sensitized OVCAR-8 and PEA1 cells to all three agents (Fig 3A–C) and upregulated NNMT (Fig. 3 bottom panels). Consistent with the observation that loss of BRCA2 and RAD51 did not disrupt OCR (Supplementary Fig. S3A and C), depletion of these HR proteins did not sensitize cells to OXPHOS inhibition (but did sensitize to the PARP inhibitor olaparib) (Supplementary Fig. S5A and B). These findings demonstrate that the metabolic reprogramming induced by BRCA1 loss sensitizes ovarian cancer cells to agents that disrupt energy metabolism and further indicate that BRCA1 regulation of metabolism is unrelated to its role in HR.

NNMT overexpression sensitizes ovarian cancer cells to mitochondrial metabolic targeting agents

Because mitochondrial metabolic defects induced by BRCA1 depletion occurred through NNMT upregulation (Fig. 2), we next asked whether NNMT overexpression was sufficient to sensitize ovarian cancer cells to mitochondrial metabolic targeting agents. To assess this possibility, we created three clones of OVCAR-8 cells that stably overexpress NNMT (Fig. 4A). As was seen with BRCA1-depletion, NNMT overexpression reduced OCR (Fig. 4A) and ATP levels (Supplementary Fig. S6A). Moreover, CDK12 or BRCA1 depletion did not further reduce ATP levels when NNMT was overexpressed (Supplementary Fig. S6A), indicating that reduced ATP levels caused by BRCA1 depletion are driven primarily by NNMT overexpression. Notably, these NNMT-induced metabolic changes were not due to reduced proliferation rate (Supplementary Fig. S6B), although BRCA1 depletion did reduce proliferation (Supplementary Fig. S6C), likely because BRCA1 has additional effects on cell proliferation (24). Consistent with reduced OCR and ATP levels (Fig. 4A; Supplementary Fig. S6A), NNMT overexpression sensitized the cells to mitochondrial metabolic targeting agents (Fig. 4B). These results demonstrate that NNMT upregulation reprograms metabolism and sensitizes ovarian cancer cells to agents that target mitochondrial metabolism without reducing proliferation.

In an attempt to understand why OXPHOS inhibitors were more cytotoxic in BRCA1-depleted and NNMT-overexpressing cells, we assessed the impact of an OXPHOS inhibitor on ATP levels in BRCA1-depleted and NNMT overexpressing OVCAR-8 cells, which already have compromised ATP levels (Supplementary Fig. S1A, S2C, and S6A). Consistent with the previous reports showing that VLX600 reduced ATP levels (7), we observed a further reduction in ATP in BRCA1-depleted as well as in NNMT overexpressing cells (Fig. 4C). These results suggest that OXPHOS inhibitors are more toxic in cells with reduced

levels of OXPHOS, possibly due to the additional metabolic stress imposed by agents such as VLX600 and other OXPHOS inhibitors (Fig. 4D).

Summary

In summary, we demonstrated here that BRCA1 deficiency, via its ability to upregulate NNMT, reprograms metabolism by reducing mitochondrial respiration. We also showed that this metabolic reprogramming sensitizes ovarian cancer cells to small molecules that disrupt energy metabolism. Interestingly, the concentrations of VLX600 that are selectively cytotoxic to BRCA1-deficient and NNMT-overexpressing cells are readily achieved in patients treated with this agent. For example, a phase 1 trial of VLX600 as a single agent found plasma C_{max} concentrations of 1–2 μ M in humans (25), well above the 30–100 nM concentrations used in the present studies (Fig. 3). Because BRCA1 dysfunction and NNMT overexpression are common features of many cancers (12), including HGSO (13,14), our findings suggest that metabolic vulnerabilities created by these tumor-associated alterations might be common and might be therapeutically targeted by agents that are FDA-approved or have been in clinical trials.

Supplementary Material

Refer to Web version on PubMed Central for supplementary material.

ACKNOWLEDGEMENTS

This work was supported by NIH (R01 CA194498 to L.M.K.), Mayo Clinic Ovarian Cancer SPORE (P50 CA136393 to S.H.K.), a Mayo Clinic Ovarian Cancer SPORE Career Enhancement Award (P50 CA136393 to A.K.), a Foundation for Women's Cancer Genentech Ovarian Cancer Young Investigator Career Development Award (to A.K.), a Wallace and Evelyn Simmers Career Development Award for Ovarian Cancer Research (to A.K.), and an infrastructure grant from the Minnesota Partnership for Biotechnology & Medical Genomics (to S.H.K.).

REFERENCES

1. Bowtell DD, Bohm S, Ahmed AA, Aspuria PJ, Bast RC Jr., Beral V, et al. Rethinking ovarian cancer II: reducing mortality from high-grade serous ovarian cancer. *Nat Rev Cancer* 2015;15:668–79 [PubMed: 26493647]
2. Joshi PM, Sutor SL, Huntoon CJ, Karnitz LM. Ovarian cancer-associated mutations disable catalytic activity of CDK12, a kinase that promotes homologous recombination repair and resistance to cisplatin and poly(ADP-ribose) polymerase inhibitors. *J Biol Chem* 2014;289:9247–53 [PubMed: 24554720]
3. Blazek D, Kohoutek J, Bartholomeeusen K, Johansen E, Hulinkova P, Luo Z, et al. The Cyclin K/ Cdk12 complex maintains genomic stability via regulation of expression of DNA damage response genes. *Genes Dev* 2011;25:2158–72 [PubMed: 22012619]
4. Lord CJ, Ashworth A. BRCAness revisited. *Nat Rev Cancer* 2016;16:110–20 [PubMed: 26775620]
5. Morgan RD, Clamp AR, Evans DGR, Edmondson RJ, Jayson GC. PARP inhibitors in platinum-sensitive high-grade serous ovarian cancer. *Cancer Chemother Pharmacol* 2018;81:647–58 [PubMed: 29464354]
6. Vander Heiden MG. Targeting cancer metabolism: a therapeutic window opens. *Nat Rev Drug Discov* 2011;10:671–84 [PubMed: 21878982]
7. Zhang XN, Fryknes M, Hernlund E, Fayad W, De Milito A, Olofsson MH, et al. Induction of mitochondrial dysfunction as a strategy for targeting tumour cells in metabolically compromised microenvironments. *Nat Commun* 2014;5:3295 [PubMed: 24548894]

8. Jackson KC, Gidlund EK, Norrbom J, Valencia AP, Thomson DM, Schuh RA, et al. BRCA1 is a novel regulator of metabolic function in skeletal muscle. *J Lipid Res* 2014;55:668–80 [PubMed: 24565757]
9. Privat M, Radošević-Robin N, Aubel C, Cayre A, Penault-Llorca F, Marceau G, et al. BRCA1 Induces Major Energetic Metabolism Reprogramming in Breast Cancer Cells. *PLoS One* 2014;9:e102438 [PubMed: 25010005]
10. Jackson KC, Tarpey MD, Valencia AP, Inigo MR, Pratt SJ, Patteson DJ, et al. Induced Cre-mediated knockdown of Brca1 in skeletal muscle reduces mitochondrial respiration and prevents glucose intolerance in adult mice on a high-fat diet. *FASEB J* 2018;32:3070–84 [PubMed: 29401626]
11. Kraus D, Yang Q, Kong D, Banks AS, Zhang L, Rodgers JT, et al. Nicotinamide N-methyltransferase knockdown protects against diet-induced obesity. *Nature* 2014;508:258–62 [PubMed: 24717514]
12. Pissios P Nicotinamide N-methyltransferase: more than a vitamin B3 clearance enzyme. *Trends Endocrin Met* 2017;28:340–53
13. Kanska J, Aspúria PJP, Taylor-Harding B, Spurka L, Funari V, Orsulic S, et al. Glucose deprivation elicits phenotypic plasticity via ZEB1-mediated expression of NNMT. *Oncotarget* 2017;8:26200–20 [PubMed: 28412735]
14. Eckert MA, Coscia F, Chryplewicz A, Chang JW, Hernandez KM, Pan S, et al. Proteomics reveals NNMT as a master metabolic regulator of cancer-associated fibroblasts. *Nature* 2019;569:723–8 [PubMed: 31043742]
15. Wang A, Schneider-Broussard R, Kumar AP, MacLeod MC, Johnson DG. Regulation of BRCA1 expression by the Rb-E2F pathway. *J Biol Chem* 2000;275:4532–6 [PubMed: 10660629]
16. Chini CC, Chen J. Repeated phosphopeptide motifs in human Claspin are phosphorylated by Chk1 and mediate Claspin function. *J Biol Chem* 2006;281:33276–82 [PubMed: 16963448]
17. Moreno-Sanchez R, Marin-Hernandez A, Saavedra E, Pardo JP, Ralph SJ, Rodriguez-Enriquez S. Who controls the ATP supply in cancer cells? Biochemistry lessons to understand cancer energy metabolism. *Int J Biochem Cell B* 2014;50:10–23
18. Perry SW, Norman JP, Barbieri J, Brown EB, Gelbard HA. Mitochondrial membrane potential probes and the proton gradient: a practical usage guide. *Biotechniques* 2011;50:98–115 [PubMed: 21486251]
19. Konstantinopoulos PA, Ceccaldi R, Shapiro GI, D'Andrea AD. Homologous Recombination Deficiency: Exploiting the Fundamental Vulnerability of Ovarian Cancer. *Cancer Discov* 2015;5:1137–54 [PubMed: 26463832]
20. Liang K, Gao X, Gilmore JM, Florens L, Washburn MP, Smith E, et al. Characterization of human CDK12 and CDK13 complexes in CTD phosphorylation, gene transcription and RNA processing. *Mol Cell Biol* 2015;35:928–38 [PubMed: 25561469]
21. Ulanovskaya OA, Zuhl AM, Cravatt BF. NNMT promotes epigenetic remodeling in cancer by creating a metabolic methylation sink. *Nat Chem Biol* 2013;9:300–6 [PubMed: 23455543]
22. Jia XF, Gu ZF, Chen WM, Jiao JB. Tigecycline targets nonsmall cell lung cancer through inhibition of mitochondrial function. *Fund Clin Pharmacol* 2016;30:297–306
23. Liu Y, Cao YY, Zhang WH, Bergmeier S, Qian YR, Akbar H, et al. A small-molecule inhibitor of glucose transporter 1 downregulates glycolysis, induces cell-cycle arrest, and inhibits cancer cell growth in vitro and in vivo. *Mol Cancer Ther* 2012;11:1672–82 [PubMed: 22689530]
24. Deng CX. BRCA1: cell cycle checkpoint, genetic instability, DNA damage response and cancer evolution. *Nucleic Acids Res* 2006;34:1416–26 [PubMed: 16522651]
25. Mody K, Mansfield AS, Vemireddy L, Nygren P, Gulbo J, Borad M. A phase I study of the safety and tolerability of VLX600, an iron chelator, in patients with refractory advanced solid tumors. *Invest New Drugs* 2019;37:684–92 [PubMed: 30460505]

Significance

Loss of BRCA1 reprograms metabolism creating a therapeutically targetable vulnerability in ovarian cancer

Author Manuscript

Author Manuscript

Author Manuscript

Author Manuscript

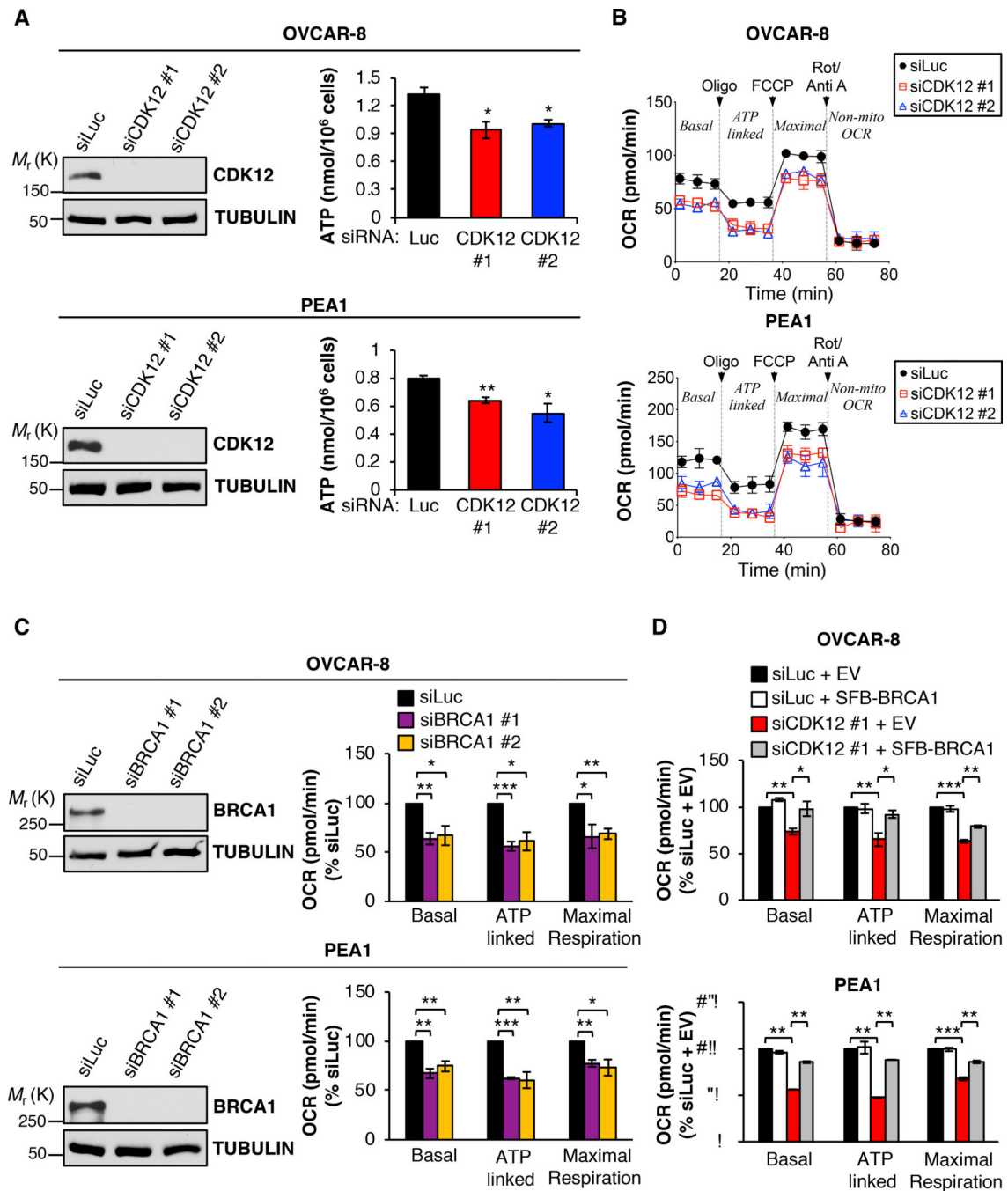


Figure 1. CDK12 depletion downregulates BRCA1, which causes decreased ATP levels and suppresses mitochondrial respiration.

(A) Analysis of ATP levels in CDK12-depleted cells. OVCA8-8 (*top panel*) and PEA1 (*bottom panel*) cells were transfected with control luciferase (siLuc) or CDK12 siRNAs (siCDK12 #1 and siCDK12 #2). 48 h after transfection, ATP levels were measured (*right panels*), and CDK12 and tubulin levels were analyzed by immunoblotting (*left panels*). Data are means \pm SEM, $n = 3$ independent experiments. * $P < 0.05$, ** $P < 0.01$, unpaired t test.

(B) Effect of CDK12 depletion on oxygen consumption rate (OCR). OVCA8-8 or PEA1

cells were transfected with control siLuc or CDK12 siRNAs. 48 h later, OCRs were measured under basal conditions and following the sequential additions of oligomycin, FCCP, and rotenone/antimycin A using a Seahorse XFp extracellular flux analyzer. Data are representative of 3 independent experiments. **(C)** BRCA1 depletion also disrupts OCR. OVCAR-8 and PEA1 cells were transfected with control siLuc or BRCA1 siRNAs (siBRCA1 #1 and siBRCA1 #2). 48 h later, BRCA1 and TUBULIN were analyzed by immunoblotting (*left panels*), and OCR was measured as described in **B** (*right panels*). Data are means \pm SEM, n = 3 independent experiments. *P < 0.05, **P < 0.01, ***P < 0.001, unpaired *t* test. **(D)** Ectopic BRCA1 expression rescues the OCR defect induced by BRCA1. OVCAR-8 (top panel) and PEA1 (bottom panel) cells were transfected with siLuc or CDK12 siRNAs plus empty vector (EV) or SFB-BRCA1 plasmid (SFB-BRCA1). OCR was measured as described in **B**. Data are means \pm SEM, n = 3 independent experiments. *P < 0.05, **P < 0.01, ***P < 0.001, unpaired *t* test.

Author Manuscript

Author Manuscript

Author Manuscript

Author Manuscript

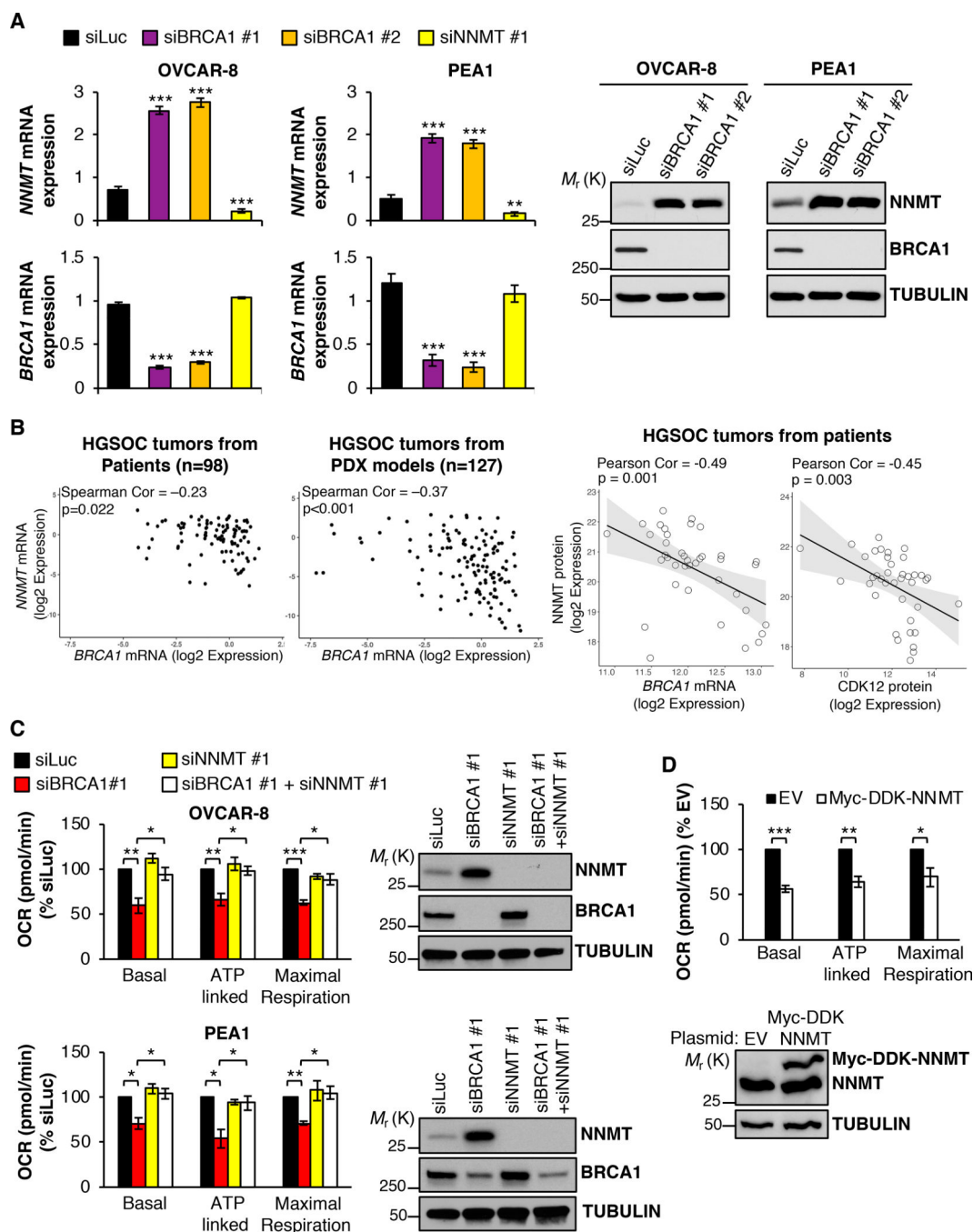


Figure 2. BRCA1 depletion induces NNMT upregulation, which causes decreased OCR.

(A) OVCAR-8 and PEA1 cells were transfected with control luciferase (siLuc), BRCA1, or NNMT siRNAs. 48 h later, the cells were analyzed by qPCR for *NNMT* and *BRCA1* mRNA levels, which are expressed relative to *GAPDH* mRNA levels as an internal control (left panels) and immunoblotted for NNMT, BRCA1, and tubulin (right panel). Data are means \pm SEM, $n = 3$ independent experiments. ** $P < 0.01$, *** $P < 0.001$, unpaired t test. (B) BRCA1 and CDK12 mRNA and protein levels are inversely correlated with NNMT mRNA and protein. Scatter plots of *NNMT* mRNA expression as a function of *BRCA1* and *CDK12*

mRNA expression in HGSOC tumors from patients and PDX models (*left two panels*). Scatter plots of NNMT protein as a function of *BRCA1* mRNA and CDK12 protein levels in HGSOC tumors from patients. Spearman or Pearson correlations are shown in the images. **(C)** Co-depletion of NNMT reverses the OCR defect induced by *BRCA1* depletion. OVCAR-8 (*top panel*) and PEA1 (*bottom panel*) cells were transfected with siLuc, *BRCA1*, or NNMT siRNAs individually or co-transfected with *BRCA1* and NNMT siRNAs. OCR was measured as described in Fig. 1B and NNMT, *BRCA1*, and tubulin levels were measured by immunoblotting. Data are means \pm SEM, $n = 3$ independent experiments. * $P < 0.05$, ** $P < 0.01$, *** $P < 0.001$, unpaired t test. **(D)** NNMT overexpression phenocopies the OCR defect induced by *BRCA1* depletion. OVCAR-8 cells were transiently transfected with empty vector (EV) or a plasmid that expresses Myc-DDK-tagged NNMT. After 24 h, OCR was analyzed as described in Fig. 1B and cells were immunoblotted for NNMT and tubulin. Data are means \pm SEM, $n = 3$ independent experiments. * $P < 0.05$, ** $P < 0.01$, *** $P < 0.001$, unpaired t test.

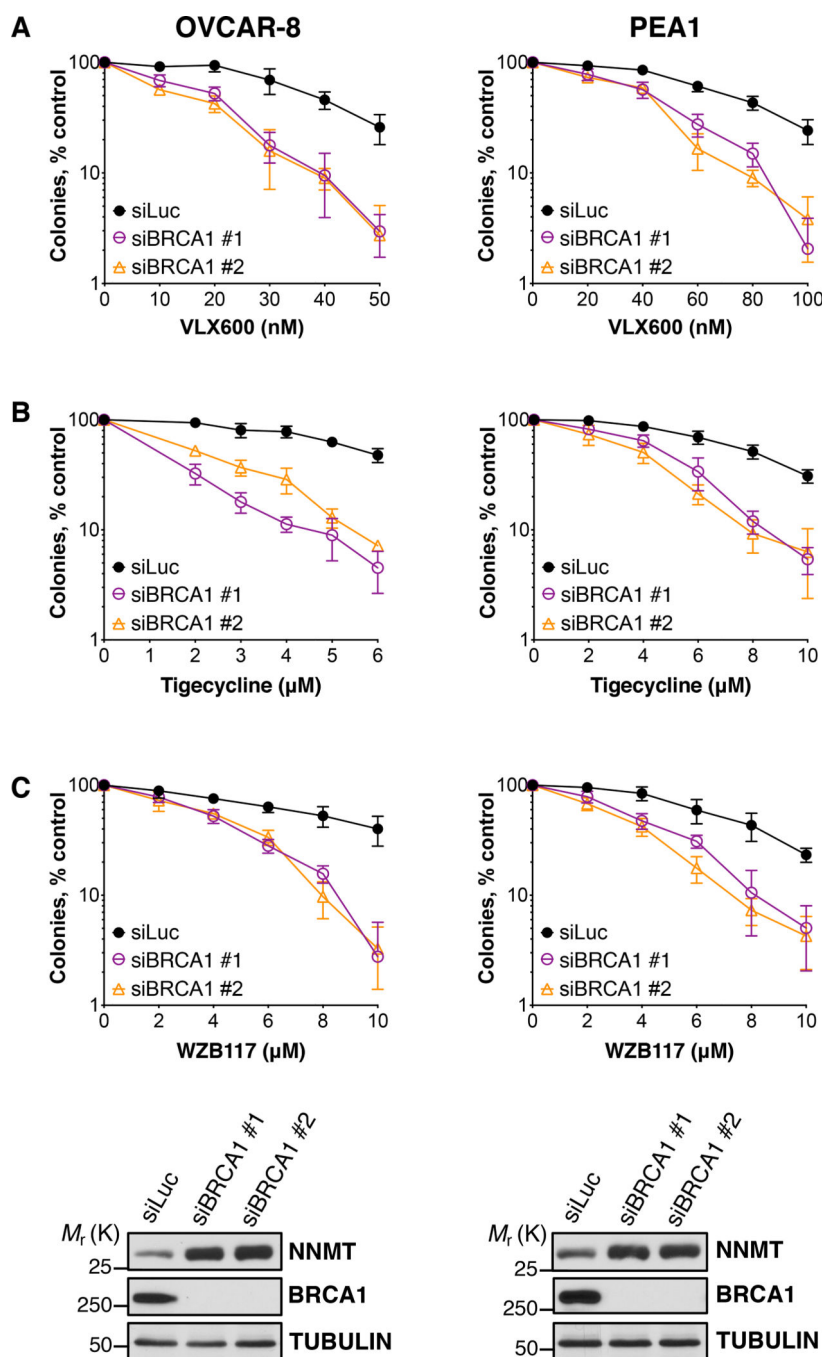


Figure 3. BRCA1 depletion sensitizes ovarian cancer cells to agents that disrupt metabolism. (A-C) OVCAR-8 and PEA1 cells were transfected with control luciferase (siLuc) or BRCA1 siRNAs. 48 h later, the cells were trypsinized, immunoblotted for BRCA1 and tubulin (*bottom panels*), and subjected to colony formation assays. The indicated concentrations of VLX600 (A), tigecycline (B), or WZB117 (C) were added 12 h after plating, and the cells were cultured for 8–10 days to allow colony formation. Data are representative of 3 independent experiments. Error bars: means \pm SEM of three technical replicates in the representative experiment.

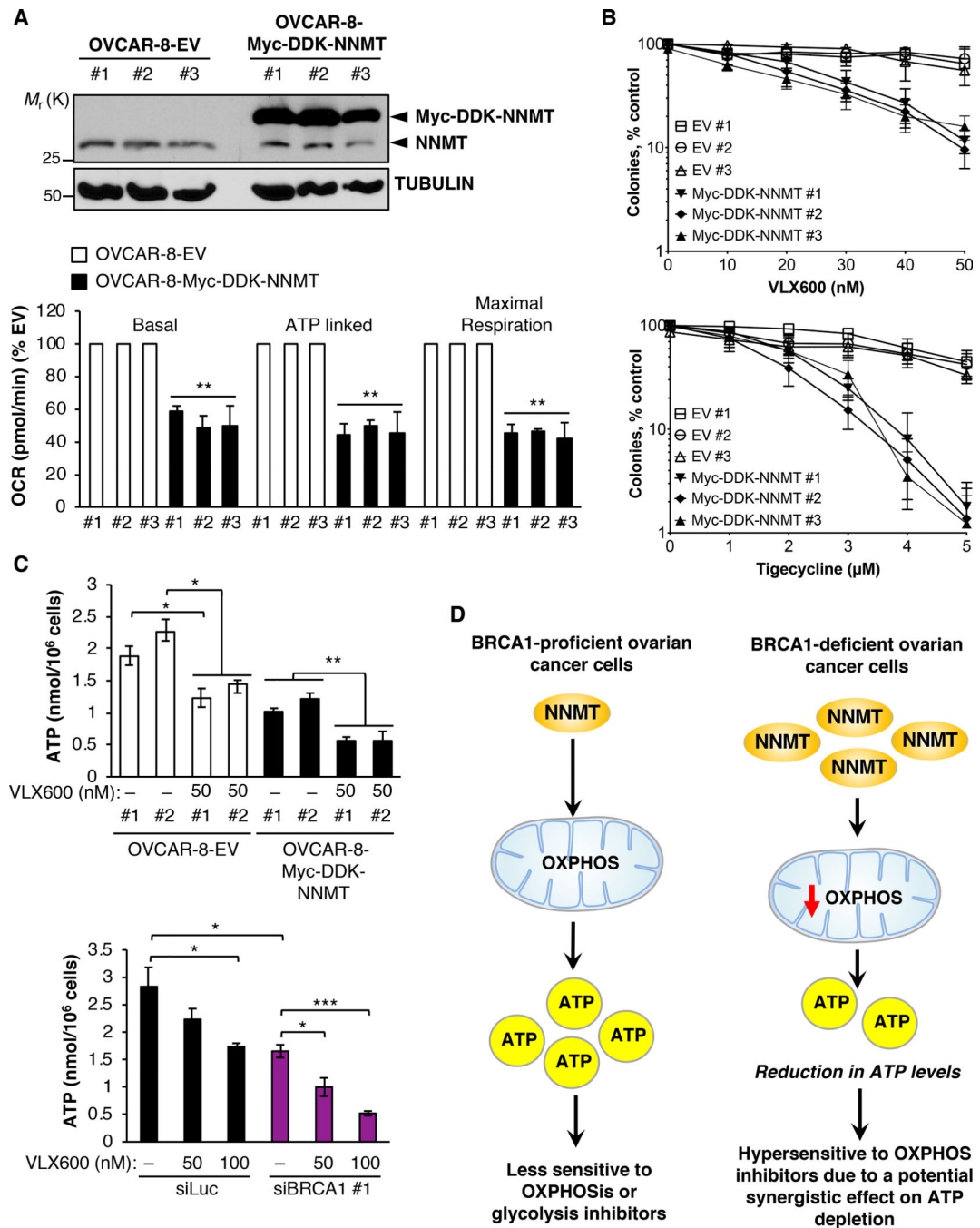


Figure 4. NNMT overexpression sensitizes ovarian cancer cells to agents that disrupt metabolism.

(**A** and **B**) Clones of OVCAR-8 cells stably transfected with empty vector (pcDNA3) or the Myc-DDK-NNMT expression plasmid were subjected to immunoblotting for NNMT and tubulin (**A**, *top panel*), examined for OCR as described in Fig. 1B (**A**, *bottom panel*), and treated with VLX600 (**B**, *top panel*) or tigecycline (**B**, *top panel*), which were added 12 h after plating the cells. The cells were cultured for 8–10 days to allow colony formation. Data in **A** (*bottom panel*) are means \pm SEM, $n = 3$ independent experiments, $**P < 0.01$, unpaired t test. Data in **B** are representative of 3 independent experiments. Error bars: means \pm SEM

of three technical replicates for each data point in the representative experiment. **(C)** VLX600 further reduces ATP levels in NNMT overexpressing cells (*top panel*) and BRCA1-depleted cells (*bottom panel*). Stable clones of the OVCAR-8-EV or the OVCAR-8-Myc-DDK-NNMT cells were treated with 50 nM VLX600 for 24 h, and OCR was measured as described in Fig. 1B (*top panel*). Control luciferase (siLuc)- or BRCA1 siRNA-transfected OVCAR-8 cells were treated with indicated concentrations of VLX600 for 24 h and OCR was measured (*bottom panel*) Data are means \pm SEM, n = 3 independent experiments, *P < 0.05, **P < 0.01, unpaired *t* test. **(D)** Model for the increased cytotoxic effect of metabolic inhibitors in BRCA1-deficient cells. Left panel: In BRCA1-proficient cells low NNMT levels lead to higher ATP levels so that these cells are less sensitive to metabolic inhibitors. Right panel: In BRCA1-deficient cells, NNMT levels are increased, leading to reduction in OXPHOS and ATP levels. These cells are more sensitive to OXPHOS inhibitors, because they are already metabolically stressed and unable to meet their energy demands when challenged with inhibitors that further reduce ATP levels.